

# Tomographic Reconstruction of Imaging Diagnostics with a Generative Adversarial Network

Naoki KENMOCHI, Masaki NISHIURA<sup>1</sup>), Kaori NAKAMURA and Zensho YOSHIDA

*The University of Tokyo, Kashiwa 277-8561, Japan*

<sup>1</sup>*National Institute for Fusion Science, Toki 509-5292, Japan*

(Received 8 May 2019 / Accepted 20 May 2019)

We have developed a tomographic reconstruction method using a conditional Generative Adversarial Network to obtain local-intensity profiles from imaging-diagnostic data. To train the network we prepared pairs of local-emissivity and line-integrated images that simulate the experimental system. After validating the accuracy of the trained network, we used it to reconstruct a local image from a measured line-integrated image. We applied this procedure to the He II-emission imaging diagnostic for RT-1 magnetospheric plasmas, including the effects of stray light within the measured image to remove reflections from the chamber walls in the reconstruction. The local intensity profiles we obtain clearly elucidate the effect of ion-cyclotron-resonance heating. This method is a powerful tool for systems where it is difficult to solve the inversion problem due to the involved contributions of nonlocal optical effects or measurement restrictions.

© 2019 The Japan Society of Plasma Science and Nuclear Fusion Research

Keywords: deep learning, generative adversarial network, imaging diagnostic, tomographic reconstruction, laboratory magnetosphere

DOI: 10.1585/pfr.14.1202117

Imaging diagnostics play key roles in analyzing the internal structures of plasmas in which it is impossible to insert detectors for avoiding damages in plasmas and/or diagnostics. Conventional tomography employs a simple model of internal structure, and the model parameters are easily evaluated by inverting the integrated observables. For a more general system, however, one requires more-involved models that are not easily solvable. The limited accessibility of diagnostics or the influence of nonlocal optical effects (such as backscatter from the chamber walls) can cause a lack of data, resulting in numerical instabilities in the inversion problem. To overcome this problem, deep-learning convolutional neural networks (CNNs) have been applied at JET to reconstruct the 2D plasma profile with satisfactory accuracy [1]. This method is even faster than classical tomographic methods, which generally need higher computational demands. A CNN learns to minimize a loss function that scores the quality of the results. Although the learning process is automatic, numerous manual processes are necessary to design an effective loss function. A Generative Adversarial Network (GAN) has been proposed to learn the loss function automatically via an adversarial process [2]. A GAN learns a loss that tries to classify whether output images are real or fake, while simultaneously training a generative model to minimize this loss. A “conditional GAN” (cGAN) learns a conditional generative model, applying the same generic approach to problems that would traditionally require very different loss formulations [3]. In the present work, we have built a method

using cGAN and used it to obtain the local emissivity from line-integrated images.

We applied this reconstruction technique to the He II 468.6 nm imaging diagnostic of Coherence Imaging Spectroscopy (CIS) [4] from RT-1, a laboratory magnetosphere created by levitating a superconducting ring magnet [5]. To train the network to reconstruct images, we generated pairs of local-intensity profiles and line-integrated images that simulate the optics of the CIS system. We generated the local emissivity using typical model functions for the electron-density and temperature profiles of RT-1, which are given as functions of the magnetic-flux surface [6]. We generated the line-integrated images from the local emissivity, assuming toroidal symmetry for the RT-1 plasmas. We took account of reflections from the chamber walls and the levitation magnet (L-magnet). We also employed the CIS optics to simulate the results, using the optical-engineering program ZEMAX. In that calculation, we used the TensorFlow 1.13.1 implementation of cGAN named “pix2pix” [3]. This implementation uses modules of the form convolution-BatchNorm-ReLu [7, 8] for both generator and discriminator. We selected a total of 6500 pairs of images randomly as input for the training, which spanned one million iterations. We also generated another set of 1300 samples using the same strategy, which we employed as a validation set to avoid overfitting. Figure 1 shows three sets of input, output, and target images for the network. Note that this particular reconstruction was not part of either the training set or the validation set. To quantify the differences between each pair of reconstructions,

author's e-mail: kenmochi@ppl.k.u-tokyo.ac.jp

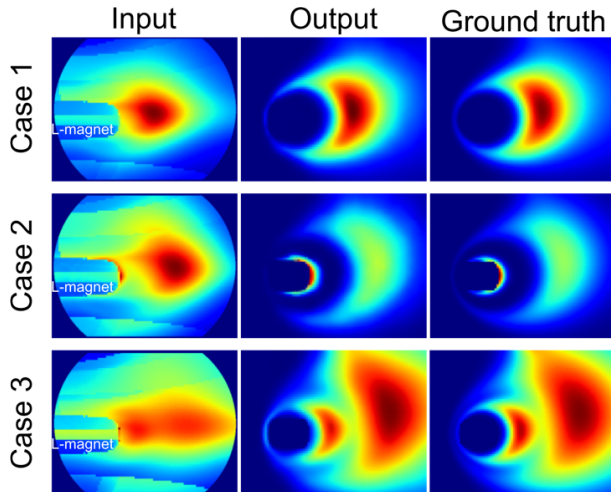


Fig. 1 Sample reconstructions produced by the network. The line-integrated image (Input, left), reconstructed local emissivity (Output, middle), and target image (Ground truth, right).

Table 1 Quality Metrics for the 1300-pair Validation Set.

	SSIM	NRMSE	PSNR [dB]
Mean	0.9393	0.0631	25.957
Std. dev.	0.0224	0.0165	2.546

we used image-quality metrics such as structural similarity (SSIM) [9], peak signal-to-noise ratio (PSNR) [10], and normalized root-mean-square error (NRMSE) [11]. Here, SSIM reaches a maximum value of 1.0 when the two images are equal (Note that one can recognize the difference between two images if the SSIM value is less than 0.9). Table 1 shows typical results for the 1300-pair validation set obtained with these metrics. They show that the network can produce reconstructions with high accuracy, as indicated by the SSIM of about 0.94, NRMSE of about 0.063, and PSNR of about 26 dB.

Once the network was trained, we applied it to images obtained by the CIS from RT-1. For helium plasmas, the CIS measured the spectral intensity, ion temperature, and flow velocity of  $\text{He}^+$ . We successfully demonstrated ion-cyclotron-resonance-frequency (ICRF) heating of magnetospheric plasmas [12]. The 10 kW input power of electron-cyclotron heating (ECH) sustained the target plasma. We applied 9.4 kW of ICRF heating to the double-loop antenna 0.1 sec after the start of the ECH injection and maintained it up to the termination of the discharge. We measured the CIS for an exposure time of 0.8 sec in the stable-density period. Figure 2 shows the reconstructed images of local  $\text{He}^+$  intensity for these plasmas. The  $\text{He}^+$  intensity increases, especially along the magnetic field lines near the L-magnet. This result corresponds that

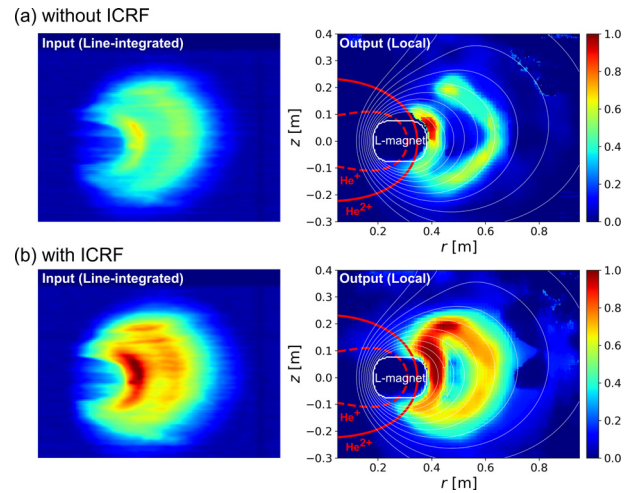


Fig. 2 Line-integrated emission intensity of CIS (left) and reconstructed local-intensity profiles (right) (a) without ICRF and (b) with ICRF. The ion cyclotron layers for  $\text{He}^{2+}$  and  $\text{He}^+$  are also shown.

the heated  $\text{He}^+$  ions around the double-loop antenna on the high-field side near the center stack move to the upper region of the L-magnet along the magnetic field lines.

In summary, we have developed a new tomography method using a cGAN and have demonstrated its efficiency by converting a line-integrated image into local emissivity. Calculation of the line-integrated image from the local emissivity is generally easier than the calculation of the opposite relation. In the present work, we have taken into account backscattering from the chamber walls, which makes even the line-integrals involved; hence conventional inversion methods do not apply. This method can be applied to other diagnostics in other machines where reconstruction is difficult because of restrictions on measurements or complexities of the inversion problem.

This work was supported by the NIFS Collaboration Research Program (Nos. NIFS15KOA034 and NIFS19KBAR026) and JSPS KAKENHI Grant Nos. 17H01177 and 18K13525.

- [1] D.R. Ferreira *et al.*, Fusion Sci. Technol. **74**, 47 (2018).
- [2] I. Goodfellow *et al.*, in Proc. NIPS, 2672 (2014).
- [3] P. Isola *et al.*, arXiv:1611.07004 (2016).
- [4] K. Nakamura *et al.*, Rev. Sci. Instrum. **89**, 10D133 (2018).
- [5] Z. Yoshida *et al.*, Phys. Rev. Lett. **104**, 235004 (2010).
- [6] M. Nishiura *et al.*, Nucl. Fusion **59**, 096005 (2019).
- [7] S. Ioffe and C. Szegedy, In ICML (2015).
- [8] A. Radford *et al.*, In ICLR (2016).
- [9] Z. WANG *et al.*, IEEE Trans. Image Process. **13**, 4, 600 (2004).
- [10] Q. Huynh-Thu and M. Ghanbari, Electron. Lett. **44**, 13, 800 (2008).
- [11] J.R. Fienup, Appl. Opt. **36**, 32, 8352 (1997).
- [12] M. Nishiura *et al.*, Nucl. Fusion **57**, 086038 (2017).